

1 **Supporting Information**

2 Article title: Tree crown damage and its effect on carbon cycling in a tropical forest

3 Authors: J. F. Needham, G. Arellano, S. J. Davies, R. A. Fisher, V. Hammer, R. Knox, D. Mitre, H.  
4 C. Muller-Landau, D. Zuleta, C. D. Koven

5  
6  
7

8 The following Supporting Information is available for this article:

9

10 **Methods S1** Recovery algorithm

11 **Methods S2** Sensitivity analyses

12 **Methods S3** Estimates of damage class from field data

13

14 **Fig. S1** Cohort splitting and fusion schematic.

15 **Fig. S2** Damage-dependent mortality as a function of the r and p parameters.

16 **Fig. S3** Ratio of leaf to stem + root respiration in FATES ensemble relationship with carbon  
17 starvation mortality.

18 **Fig. S4** Simulated size distributions under four damage scenarios.

19 **Fig. S5** Annual growth rate by damage class and canopy layer in FATES simulations and  
20 observations from BCI.

21 **Fig. S6** Size-dependent growth rates by damage class in a two PFT simulation (s5) with low and  
22 high recovery.

23 **Fig. S7.** Sensitivity to the number of crown damage classes (s8).

24 **Fig. S8** Carbon starvation mortality in small trees as a function of allocation to storage carbon  
25 (s9).

26 **Fig. S9** Leaf and stem + root respiration in FATES ensemble and observations.

27 **Fig. S10** Sensitivity of AGB and carbon residence time to damage and recovery rates (s11).

28 **Fig. S11** Sensitivity of damage-driven canopy turnover as a function of damage and recovery  
29 rate (s11).

30 **Fig. S12** Mortality by crown damage class in the damage and mortality simulation (s4).

31

32

33 **Table S1.** Additional model configurations.

34

35

36

37

38

39

40

41

42

### 43 **Methods S1** Recovery algorithm

44

45 Recovery is calculated during daily allocation. It occurs after cohorts have used NPP to replace  
46 maintenance turnover of leaves and fine roots, and once all carbon pools are at their allometric targets.  
47 At this point cohorts can either use excess carbon to grow all pools including DBH along the current,  
48 damaged, allometric trajectories, or they can use excess carbon to increase carbon pools to the  
49 allometric targets of a lesser damaged class, at the expense of DBH growth. The recovery scalar  
50 parameter,  $f_r$ , determines the fraction of the cohort that recovers when carbon is available to do so. If  $0$   
51  $< f_r < 1$ , then the cohort is split and some fraction remains in the current damage class  $d$ , while some  
52 fraction moves to damage class  $d_{-1}$ . Available carbon at the start of recovery is given by  $C_b$ .

53

54 The carbon pools for a cohort in damage class  $d$  are given by :

55  $C_{l,d}$  = leaf carbon

56  $C_{fr,d}$  = fine root carbon

57  $C_{sw,d}$  = sapwood carbon

58  $C_{str,d}$  = structural carbon

59  $C_{sto,d}$  = storage carbon

60

61 The allometric target carbon pools in damage class  $d_{-1}$  are given by :

62

63  $C_{l,d-1}$  = target leaf carbon  $d_{-1}$

64  $C_{fr,d-1}$  = target fine root carbon  $d_{-1}$

65  $C_{sw,d-1}$  = target sapwood carbon  $d_{-1}$

66  $C_{str,d-1}$  = target structural carbon  $d_{-1}$

67  $C_{sto,d-1}$  = target storage carbon  $d_{-1}$

68

69 Total carbon of cohort in damage class  $d$ ,  $C_d$ , is given by

$$70 C_d = C_{l,d} + C_{fr,d} + C_{sw,d} + C_{str,d} + C_{sto,d} \quad \text{eq. 1}$$

71

72 Total carbon of cohort in damage class  $d_{-1}$ ,  $C_{d-1}$ , is given by

$$73 C_{d-1} = C_{l,d-1} + C_{fr,d-1} + C_{sw,d-1} + C_{str,d-1} + C_{sto,d-1} \quad \text{eq. 2}$$

74

75 Carbon demand for recovery,  $C_r$ , is thus

$$76 C_r = C_{d-1} - C_d \quad \text{eq. 3}$$

77

78 The maximum number of plants that can recover,  $n_{max}$ , is given by

$$79 n_{max} = C_b * n_d / C_r \quad \text{eq. 4}$$

80

81 where  $n_d$  is the number density of the cohort in damage class  $d$  and  $C_b$  is the carbon balance for the  
82 cohort, i.e. the amount of carbon available for growth or recovery.

83

84 The number of plants that recover,  $n_r$ , is given by:

$$85 n_r = n_{max} * f_r \quad \text{eq. 5}$$

86 where  $f_r$  is the recovery scalar parameter.

87

88 The per capita carbon of the newly recovered cohort is  $C_{d-1}$ , since all carbon pools are now at the  
89 allometric target for damage class  $d_{-1}$ . The total carbon for the newly recovered cohort is  $C_{d-1} * n_r$ .

90

eq. 6

91  
92 The per capita carbon of the fraction of the cohort that does not recover,  $C_{d,t+1}$ , is now  
93  $C_{d,t+1} = (C_d * n_d - (C_{d-1} * n_r)) / (n_d - n_r)$  eq. 7  
94

95 And total carbon in the cohort is  $C_{d,t+1} * (n_d - n_r)$ . eq. 8  
96  
97  
98  
99

## 100 101 **Methods S2** Additional Sensitivity Analyses 102

103  
104 **Carbon storage parameter** Carbon starvation mortality occurs in FATES when storage carbon is  
105 depleted. To test the effect of carbon storage on carbon starvation mortality in damaged trees, we ran a  
106 sensitivity analysis to the parameter which determines the allocation to storage carbon, relative to leaf  
107 carbon (s9). In this experiment we changed the allocation to storage parameter from 1.0 to 2.0 in  
108 increments of 0.1.

109  
110 An increase in the allocation to storage parameter from 1.0 to 2.0 caused a decrease in carbon  
111 starvation mortality from 21 % yr<sup>-1</sup> to 8 % yr<sup>-1</sup> in trees < 20 cm DBH with 80% crown loss. In trees > 40 cm  
112 DBH, which have much higher storage carbon, changes to the allocation to storage parameter had no  
113 effect on carbon starvation mortality, regardless of crown damage (Fig. S8).  
114

115  
116 **Root respiration parameter** We tested how changes to root nitrogen (N) stoichiometry alter the ratio of  
117 leaf to root respiration, and carbon starvation mortality across damage classes. In these simulations  
118 (s10) we increased the root N stoichiometry from its default value of 0.02900 to 0.03300, 0.04125,  
119 0.04950, 0.05775, and 0.06600 gN/gC, corresponding to 1.0, 1.25, 1.50, 1.75 and 2.00 times the leaf N  
120 stoichiometry. Observations from Amazonian forest plots reported in Malhi et al. (2009) and Doughty et  
121 al. (2014) suggest the ratio of leaf to root and stem respiration is between 0.48 and 1.02 (Fig. S9). A root  
122 N stoichiometry of 0.66 gN/gC gives a leaf to root respiration ratio of 0.86 for an undamaged tree. In the  
123 trees with 80% crown loss, carbon starvation mortality increased sharply from 3% yr<sup>-1</sup> to 34% yr<sup>-1</sup> as root  
124 N stoichiometry increased from 0.058 gN/gC to 0.066 gN/gC (Fig. S3). Carbon starvation mortality in  
125 FATES is triggered when the ratio of storage carbon to leaf carbon falls below 1. Our results suggest that  
126 this threshold is reached when root nitrogen stoichiometry reaches a critical value between 0.058 gN/gC

127 to 0.066 gN/gC. At this level of root N stoichiometry root respiration can't be met by photosynthetic  
128 capacity, leading to a depletion of storage carbon and carbon starvation mortality.

129

130

131 **Damage and recovery parameters** To better understand how damage and recovery influence carbon  
132 cycling dynamics we ran an ensemble of simulations (s11) in which we tested all combinations of five  
133 annual damage rates (0.5% yr<sup>-1</sup> to 5.0% yr<sup>-1</sup>), and five values of the parameter for the fraction of NPP  
134 used for recovery ( $f_r$ ) (0.0 to 1.0).

135

136 Decreases in AGB and carbon residence time are sensitive to the rate of damage and, to a lesser extent,  
137 recovery (Fig S10). With no recovery, an increase in the annual damage rate from 0.5% yr<sup>-1</sup> to 5% yr<sup>-1</sup>  
138 nearly halves carbon residence time from 28 years to 15 years, and decreases AGB from 11.6 kg C m<sup>-2</sup> to  
139 5.2 kg C m<sup>-2</sup>. When the annual damage rate is 5% yr<sup>-1</sup>, an increase in the recovery scalar, which sets the  
140 fraction of available carbon used for recovery versus growth within the current damage class, from 0 to  
141 1 increases carbon residence time from 15 to 17 years, and AGB from 5.2 kg C m<sup>-2</sup> to 6.6 kg C m<sup>-2</sup>.

142

143 The rate of damage also alters the canopy area disturbed each year (Fig. S11). With no recovery, an  
144 increase in damage rate from 0.5% yr<sup>-1</sup> to 5% yr<sup>-1</sup> causes the loss of crown area from damage to increase  
145 from 23.8 to 233.4 m<sup>2</sup> yr<sup>-1</sup>, going from 15% to 56% of total canopy disturbance. Canopy disturbance area  
146 is mostly insensitive to recovery; with a damage rate of 5% yr<sup>-1</sup>, an increase in the recovery scalar from 0  
147 to 1 causes the loss of crown area from damage to increase from 233.4 m<sup>2</sup> yr<sup>-1</sup> to 235.4 m<sup>2</sup> yr<sup>-1</sup>.

148

149

150 **Table S1. Crown damage bins in damage class sensitivity analysis**

Number of crown damage classes	Crown loss in each crown damage class
1	0%
2	0%, 80%
3	0, 60%, 80%
4	0%, 40%, 60%, 80%
5	0%, 20%, 40%, 60%, 80%

151

152

153

154 **Table S2. Additional model configurations.**

155

Simulation number	s8	s9	s10	s11
<b>Name</b>	Number of crown damage classes sensitivity	Carbon allocation to storage sensitivity	Root N sensitivity	Damage and recovery rate sensitivity
<b>Crown damage classes (% crown loss)</b>	See table S1	0, 20, 40, 60, 80	0, 20, 40, 60, 80	0, 20, 40, 60, 80
<b>Root N stoichiometry</b>	0.029	0.029	0.033, 0.04125, 0.0495, 0.05775, 0.066	0.066
<b>Damage</b>	Yes	Yes	Yes	Yes
<b>Carbon storage decrease with damage</b>	No	No	No	Yes
<b><math>m_d</math> term (additional damage-driven mortality)</b>	No	No	No	No
<b>Damage rate (% yr<sup>-1</sup>)</b>	1	1	1	0.5, 1.625, 2.75, 3.875, 5
<b>Recovery</b>	0	0	0	0,0.25,0.50,0.75,1.0
<b>PFTs</b>	1	1	1	1
<b>Allocation to storage</b>	1.2	1.0,1.1,1.2,1.3,1.4,1.5,1.6,1.7,1.8,1.9,2.0	1.2	1.2

156

157

158

159

160

161 **Methods S3** Estimates of damage class from field data

162

163 The relative height of the living length  $r$  is calculated as  $l/h$ , where  $h$  is target allometric height  
164 calculated from DBH. Here we use equation 7 from [\(Martinez Cano et al. 2018\)](#).

165

$$166 \quad h = \frac{58.0 * DBH^{0.73}}{21.8 + DBH^{0.73}} \quad \text{eq. 9}$$

167

168 The relative height of the base of the crown  $C_{rh}$  is calculated as  $C_h/h$  where  $C_h$  is the height of  
169 the base of the crown, here assumed to be 1.3 m. Although this is too low in large trees, it is  
170 inconsequential as the model assumes almost no biomass in branches at that height. If  $r < C_{rh}$   
171 then the fraction of biomass remaining is calculated as:

172

173

$$174 \quad AGB_f = (1 - b_f) * (1 - (1 - r)^a) \quad \text{eq. 10}$$

175

176 Where  $b_f$  is the fraction of biomass in branches, here 0.33 based on values from [\(Chambers et](#)  
177 [al. 2001\)](#) of 288 trees in the Central Amazon, and unpublished data from Duque et al of 296  
178 trees in the Colombian Amazon.  $a$  and  $b$  (below) are parameters controlling tapering, with  
179 higher values giving more abrupt tapering. We set  $a = 2.631000$  and  $b = 9.761049$ , to create  
180 smooth transitions from trunk to crown. The biomass of the damaged tree is then  $AGB_f *$   
181 target biomass.

182

183 If  $r \geq C_{rh}$  then the proportion of remaining biomass is calculated as:

184

$$185 \quad AGB_f = bole_0 + \beta * (1 - (1 - (r - C_{rh}))^b) \quad \text{eq. 11}$$

186

187 Where  $bole_0$  is calculated as

$$188 \quad bole_0 = (1 - b_f) * (1 - (1 - C_{rh})^a) \quad \text{eq. 12}$$

189

190 And  $\beta$  is

$$191 \quad \beta = \frac{(1 - bole_0)}{(1 - C_{rh}^b)} \quad \text{eq. 13}$$

192

193

194 The proportion of biomass remaining in the crown,  $AGB_c$ , is  $AGB_f - bole_0$  and the biomass of  
195 the damaged trees is simply  $AGB_f * \text{target biomass} + AGB_c * \text{target biomass} * b_f$ .

196

197 To estimate target biomass we use equation 4 from [\(Chave et al. 2014\)](#):

198

$$199 \quad AGB_{est} = 0.0673 * (\rho DBH^2 * h)^{0.976} \quad \text{eq. 14}$$

200

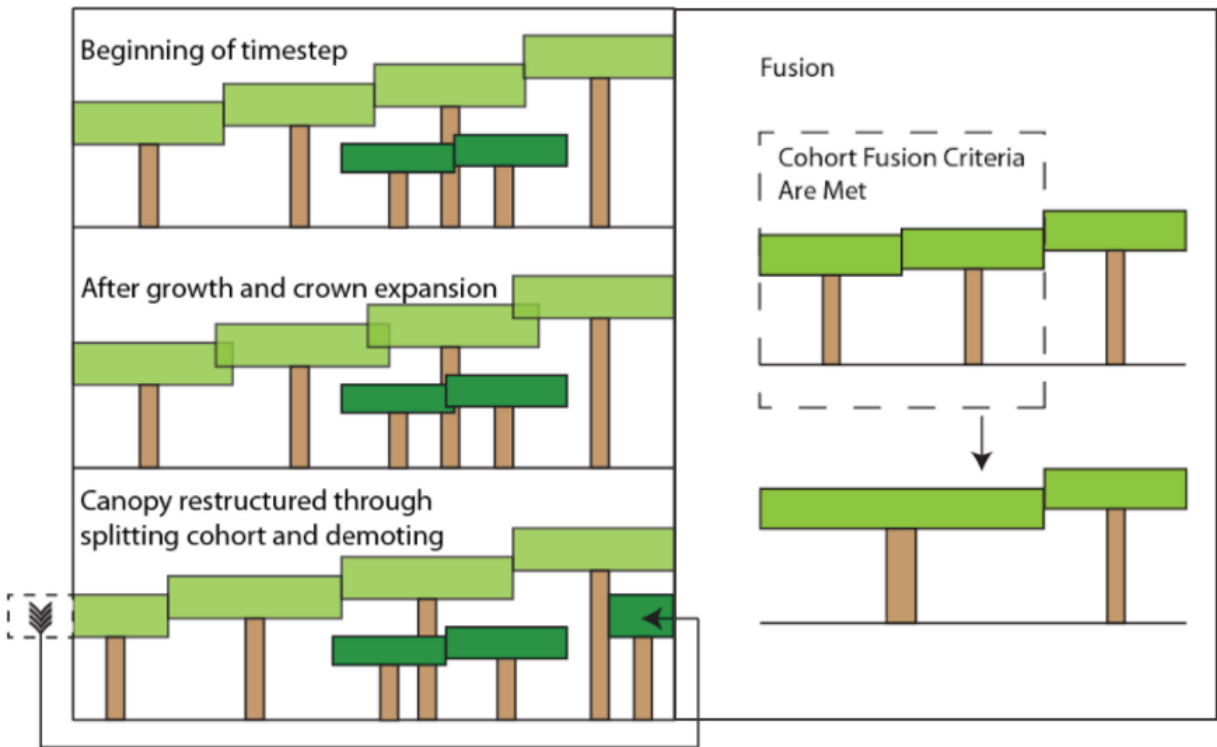
201 Where  $\rho$  is wood density, taken from [\(Zanne et al. 2009\)](#), see [\(Chave et al. 2009\)](#).

202

203 Because the damage protocol only records new damage each year, we use the cumulative  
204 product of damage loss to estimate  $b_i$  and note that this may be an underestimate of total  
205 damage in the tree.

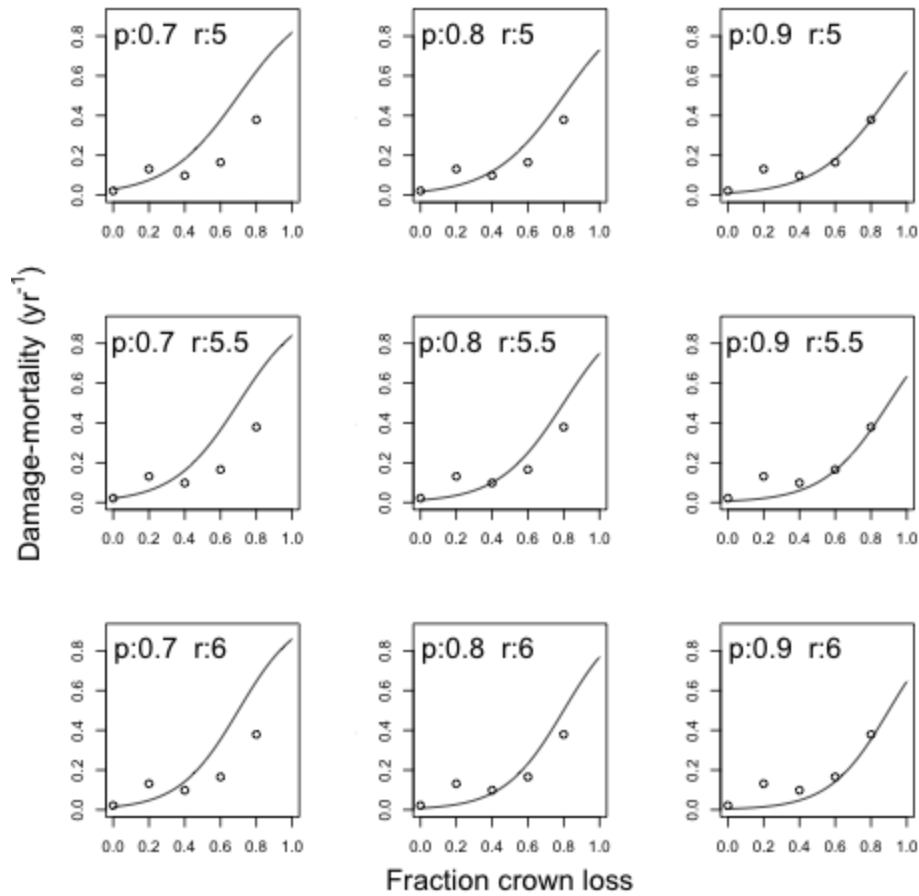
206  
207  
208  
209  
210  
211  
212

**Figures S1-S12**



213  
214  
215  
216  
217  
218  
219  
220  
221  
222  
223  
224

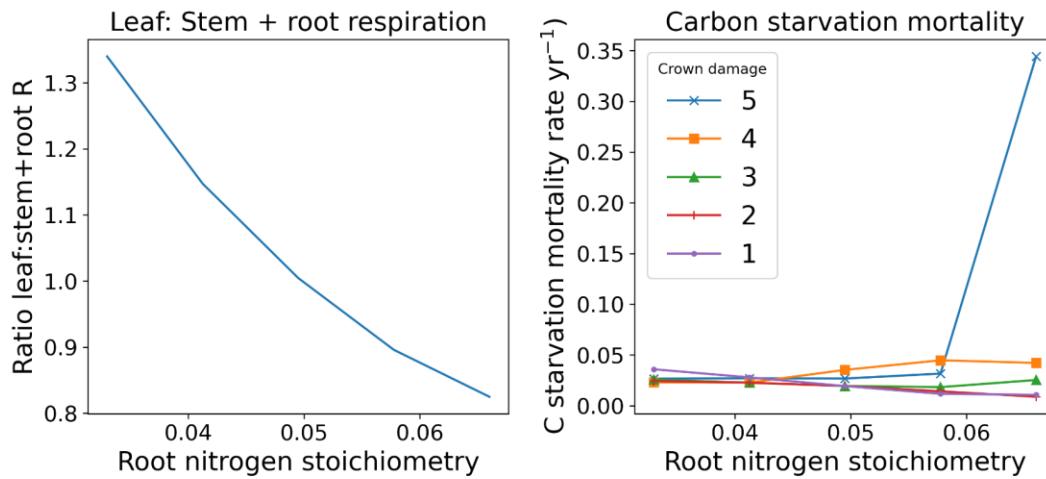
**Figure S1. Cohort splitting and fusion schematic.** The left hand panel shows cohort splitting following growth. The top panel is a patch at the beginning of the timestep. In the middle panel cohorts grow and their crowns expand. To keep total canopy area constant, in the bottom panel a fraction of the smallest cohort is demoted to the understory. This version represents the pure PPA configuration of FATES where canopy sorting is entirely deterministic. In the stochastic canopy organization configuration a fraction of all cohorts is demoted. In the right hand panel two cohorts that are within a specified dbh size threshold of one another are fused together.



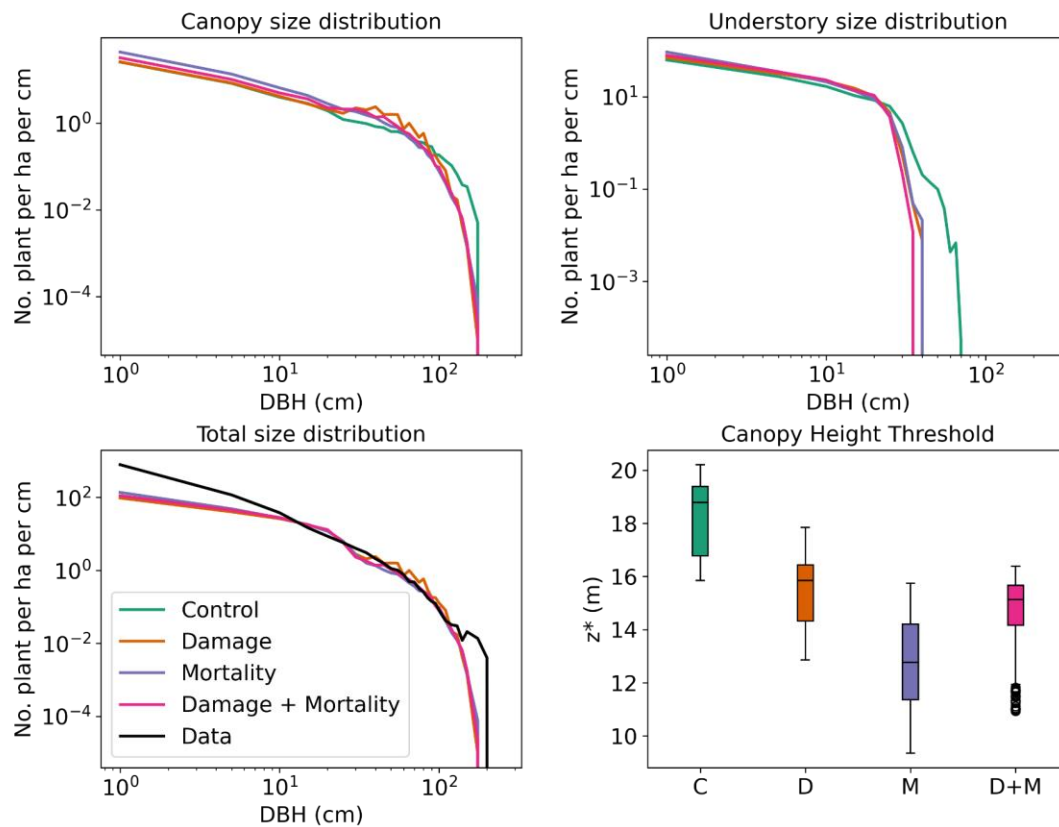
225  
 226  
 227  
 228  
 229  
 230  
 231  
 232  
 233  
 234

**Figure S2. Damage-dependent mortality as a function of the  $r$  and  $p$  parameters.** Left to right shows the effect of increasing the inflection point ( $p$ ) while top to bottom show the effect of increasing the  $r$  parameter ( $r$ ) on damage-dependent mortality. Circles show observations from damage and mortality surveys at BCI. In simulations in which this damage-dependent mortality was on, we set  $p = 0.9$  and  $r = 5.5$  (middle row, far right).



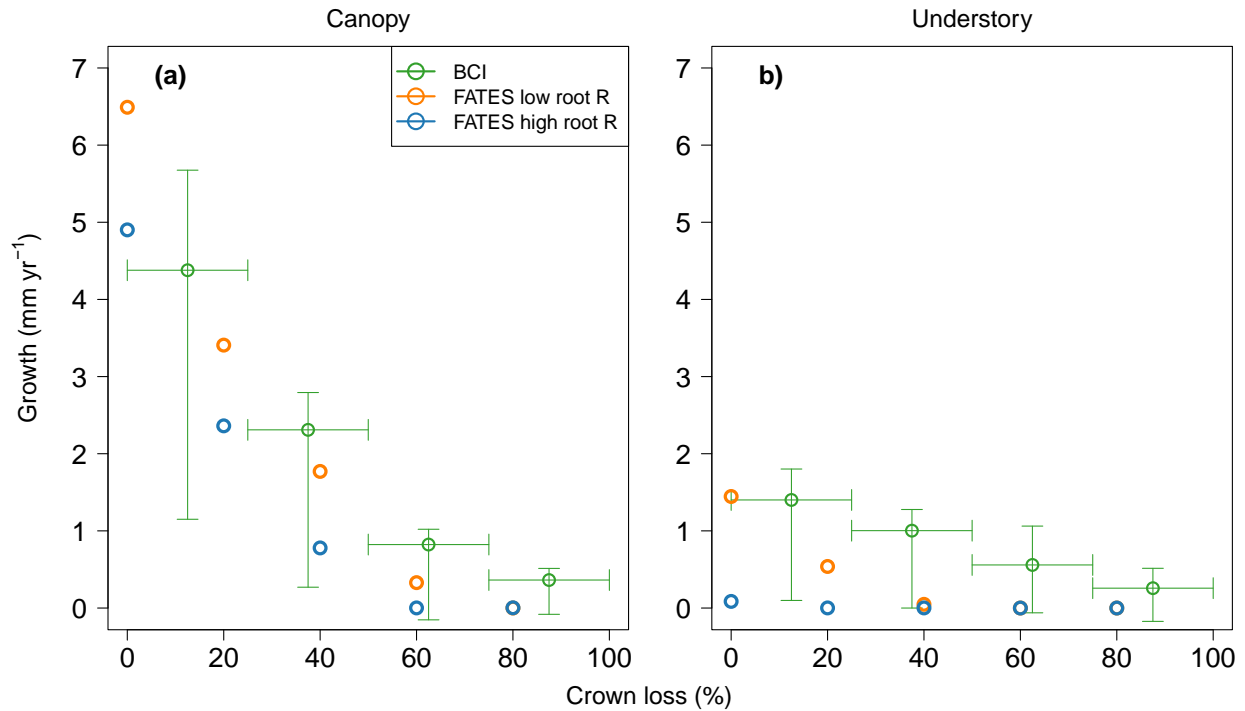


235  
 236 **Figure S3. Effects of root nitrogen stoichiometry on the simulated ratio of leaf to stem + root**  
 237 **respiration (left) and rates of carbon starvation mortality by damage class.** The left hand panel  
 238 shows the simulated ratio of total leaf to total stem + root growth and maintenance respiration  
 239 as a function of root N stoichiometry in the control model (s1). The right hand panel shows  
 240 carbon starvation mortality in each damage class as root N stoichiometry is increased. A  
 241 decrease in the ratio of leaf to stem + root respiration causes a large increase in carbon  
 242 starvation mortality in damaged trees.  
 243  
 244  
 245



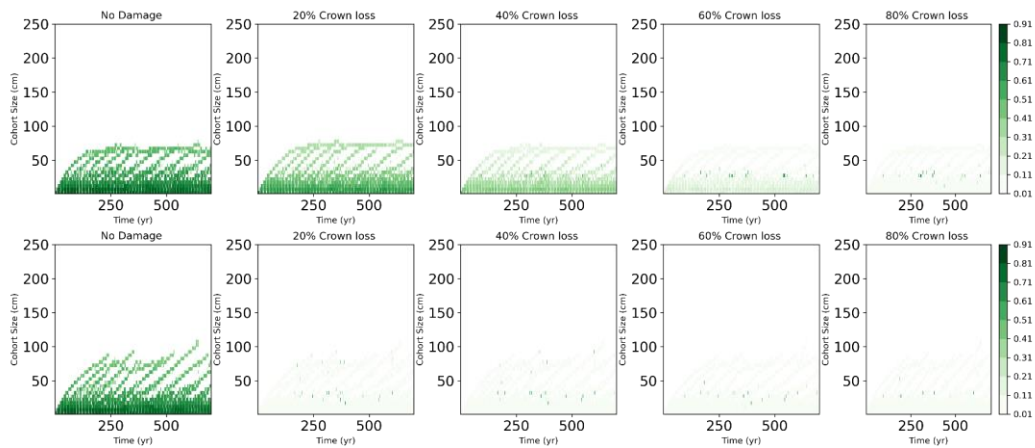
246  
 247 **Figure S4. Simulated size distributions under four damage scenarios.** The size distributions  
 248 here are the mean number of individuals per ha over the last 50 years of the simulation,  
 249 accounting for size bin width. The control simulation (C) (s1) has the damage module turned  
 250 off. The damage simulation (D) (s2) has crown damage turned on - i.e. cohorts lose crown area  
 251 and canopy biomass. In the mortality simulation (M) (s3) cohorts are split into damage classes  
 252 and are subjected to damage related mortality but do not have any reduction in crown area or  
 253 canopy biomass. In the damage + mortality simulation (D+M) (s4) cohorts have both crown  
 254 damage and damage related mortality. Simulations with damage or damage mortality have  
 255 fewer large trees in the understory since these cohorts are being promoted to the canopy due  
 256 to either increases in mortality creating canopy gaps, and/or smaller crowns in the canopy  
 257 allowing for a higher density of canopy cohorts. The bottom right panel shows the height  
 258 threshold for a cohort being in the canopy in patches over 50 years, over the last 100 years of  
 259 the simulation.

260  
 261  
 262  
 263  
 264  
 265



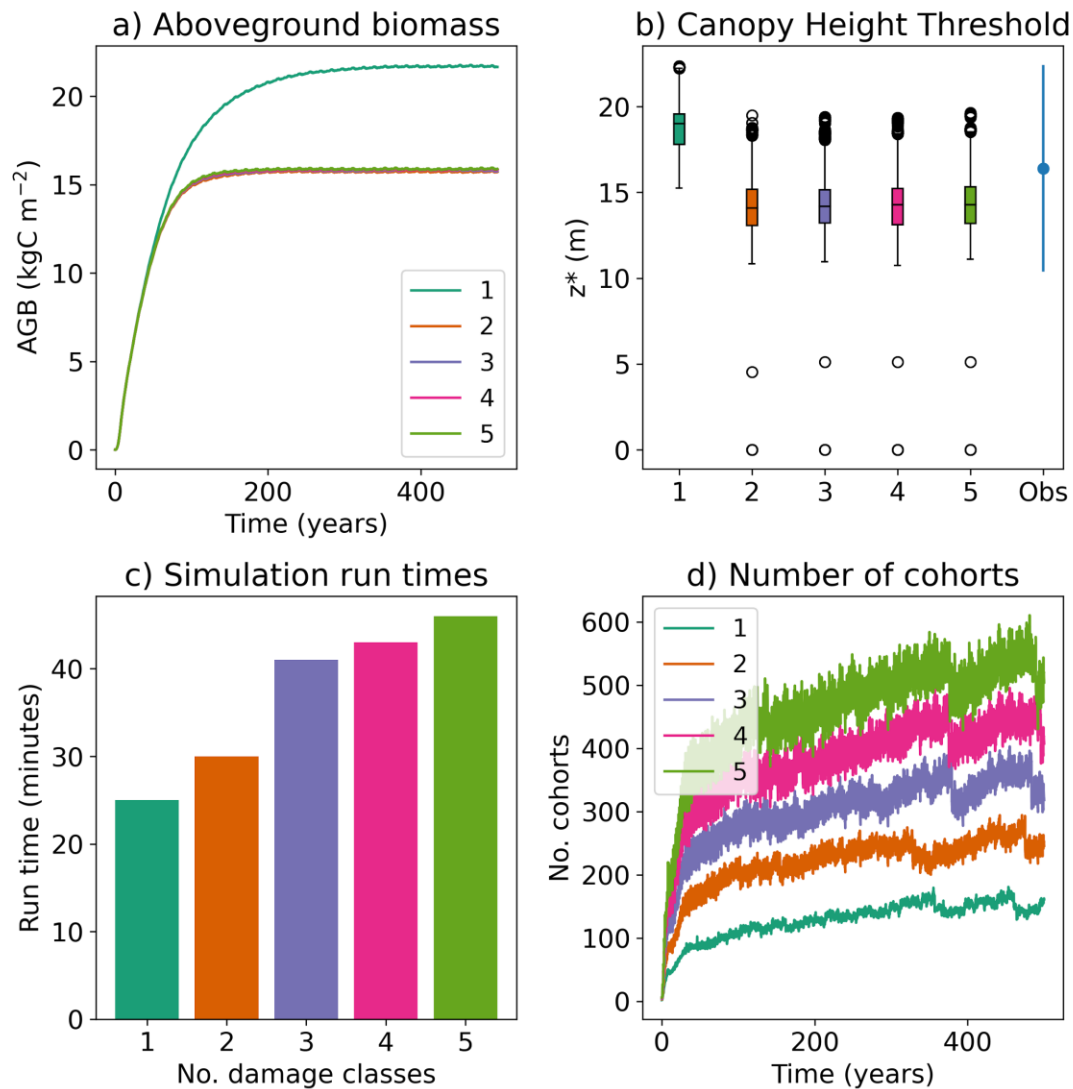
266  
 267  
 268  
 269  
 270  
 271  
 272  
 273  
 274  
 275  
 276  
 277  
 278  
 279  
 280  
 281  
 282

**Figure S5. Annual growth rate by damage class and canopy layer in FATES simulations and observations from BCI.** Orange circles show the low root N configuration of FATES (s4) and blue circles show the high root N configuration of FATES (s10). Green lines show growth rates from dendrometer band data at BCI, divided into canopy and understory. Error bars show the 50th percentile of growth rates across five census intervals. Note that damage classes in the observations are different than in FATES simulations, and hence points are offset. Damage classes in the observations include trees with a range of crown loss shown with horizontal lines, whereas in FATES damage classes correspond to a fixed percentage of crown loss. In the observational data from BCI trees with > 50% liana cover are excluded. See Fig. 5 for a version of this figure in which trees with high liana load are included.



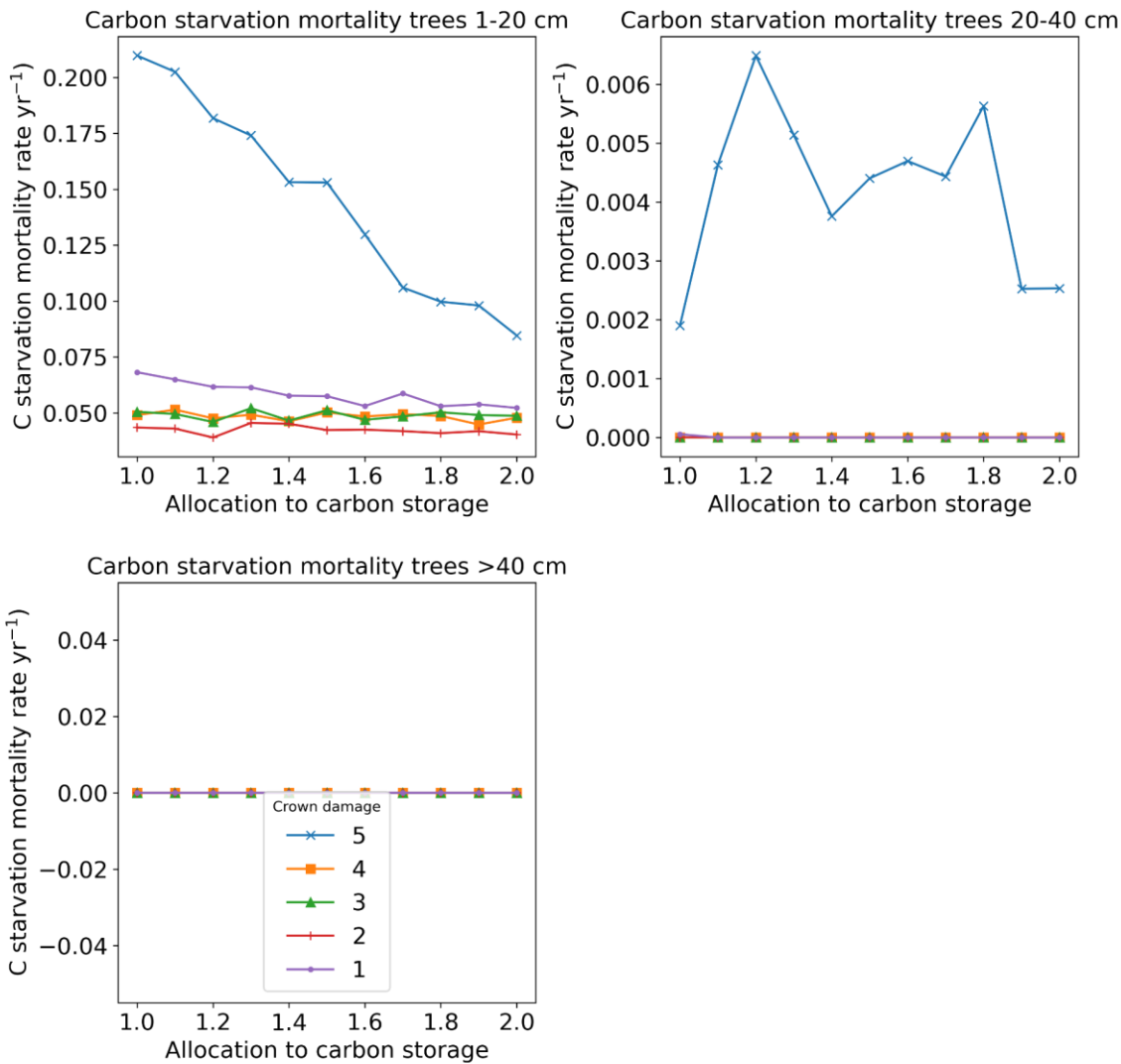
283  
 284 **Figure S6. Size-dependent growth rates by damage class in a two PFT simulation (s5) with low**  
 285 **and high recovery.** When recovery is 1 (bottom row) NPP is used to re-grow canopy tissues at  
 286 the expense of DBH growth. When recovery is 0 (top row) DBH growth is higher, but still  
 287 declines with increasing crown loss.

288  
 289  
 290

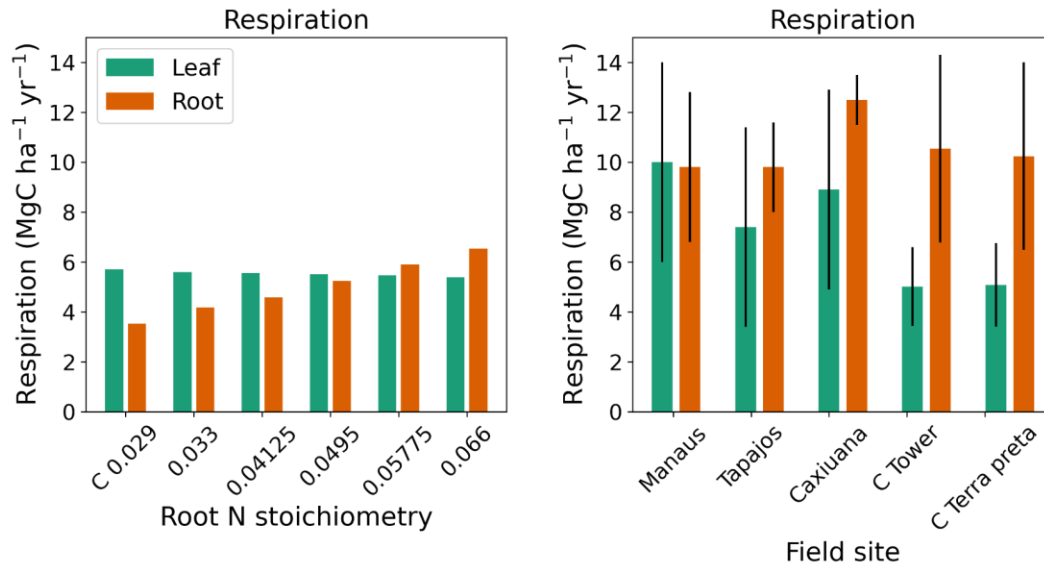


291  
 292  
 293  
 294  
 295  
 296  
 297  
 298  
 299  
 300  
 301  
 302

**Figure S7. Sensitivity to the number of crown damage classes (s8).** One damage class corresponds to only healthy trees (damage module off). Simulations with damage on always include an 80% crown loss class, with additional crown damage classes corresponding to lower levels of crown loss (see table S1). Aboveground biomass (a) and canopy height threshold (b) are lower in simulations with crown damage than in the control, but are unaffected by the number of crown damage classes. Simulation run times, here the time in minutes for the last 25 years of the simulation to run, increase with increasing numbers of damage classes (c), due to an increase in the number of cohorts to be tracked (d).

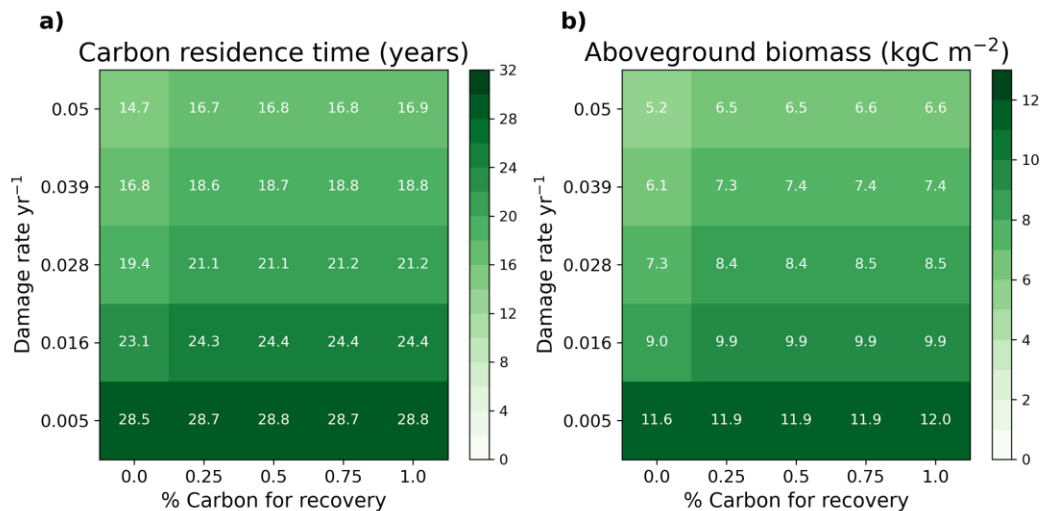


303  
 304 **Figure S8. Carbon starvation mortality as a function of allocation to storage carbon (s7).** In  
 305 large trees (>40 cm) carbon starvation mortality was independent of allocation to storage  
 306 carbon or the degree of damage. In small trees (between 1 and 40 cm DBH) with 80% crown  
 307 loss increased allocation of carbon to storage led to decreased carbon starvation mortality.  
 308



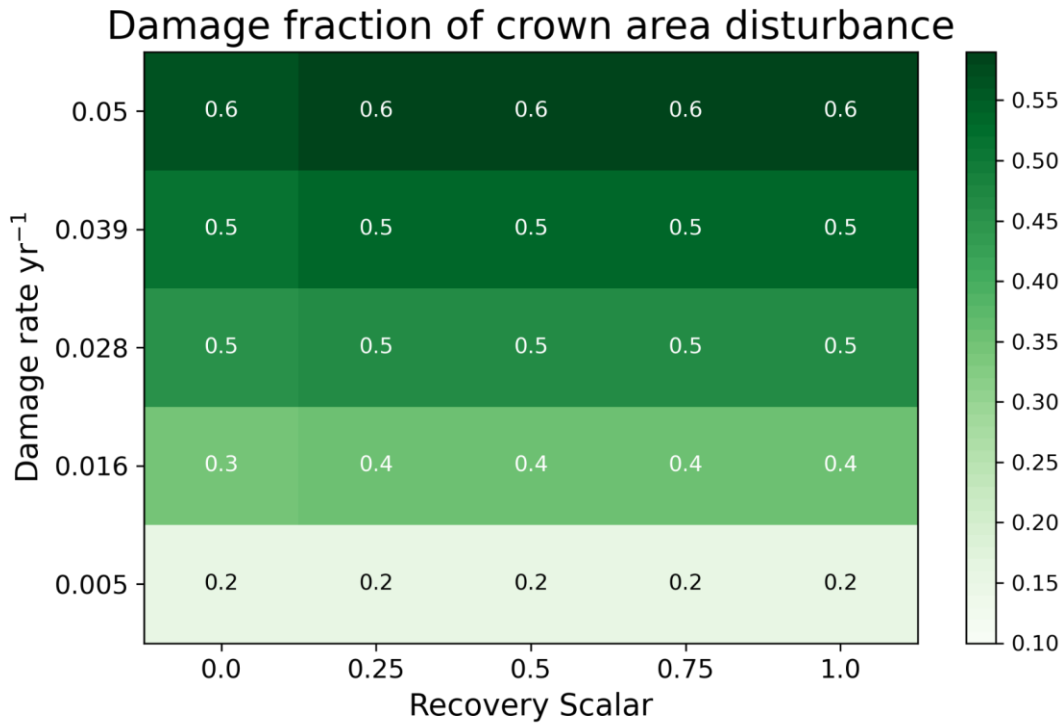
309  
 310 **Figure S9. Leaf and stem + root respiration in FATES ensemble and observations.** The left hand  
 311 panel shows growth and maintenance respiration from an ensemble (s10) in which root N  
 312 stoichiometry was increased from 0.033 to 0.066. The two left bars show a control (C) with the  
 313 default parameterisation in FATES. The right hand panel shows values from [Malhi et al. \(2009\)](#)  
 314 [and Doughty et al. \(2014\)](#). FATES underestimates stem and root respiration in all ensemble  
 315 members although the ratio of leaf to stem and root respiration in the final ensemble member  
 316 (with root N stoichiometry of 0.066) is within the range of the data.

317  
 318  
 319  
 320



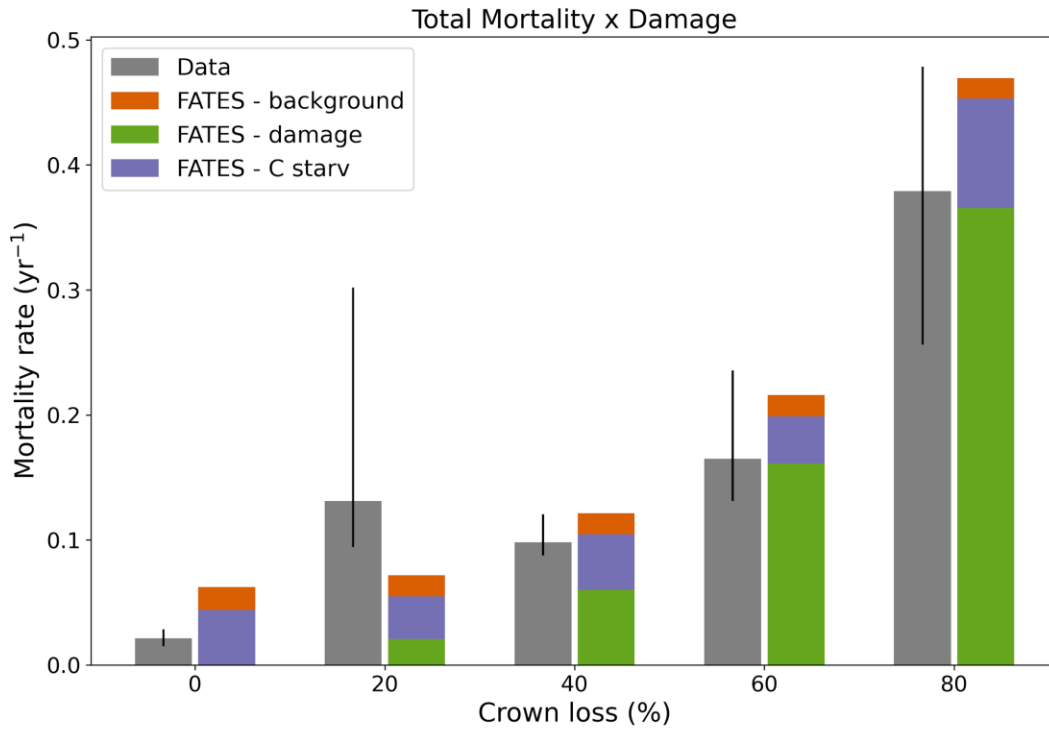
321  
 322 **Figure S10. Sensitivity of AGB and carbon residence time to damage and recovery rates (s11).**  
 323 The recovery scalar determines the fraction of available carbon that goes towards recovery  
 324 versus growth within the current damage class. The damage rate determines the fraction of

325 each cohort that is damaged each year. As the damage rate increases both carbon residence  
 326 time a) and AGB b) decrease. In contrast, as the recovery scalar increases, and more cohorts  
 327 recover, both carbon residence time and AGB increase.  
 328



329 **Figure S11. Fraction of canopy turnover from damage as a function of damage and recovery**  
 330 **rate (s11).** The proportion of canopy turnover from damage versus mortality increases as  
 331 damage fraction and recovery scalar parameters increase. The fraction of canopy turnover from  
 332 damage is most similar to observations at BCI when damage rate is  $0.005 \text{ yr}^{-1}$  and recovery  
 333 scalar is 1.  
 334  
 335  
 336





337  
 338 **Figure S12. Mortality by crown damage class in empirical data and in the damage and**  
 339 **mortality simulation (s4).** Annual mortality from observations at BCI are shown with grey bars.  
 340 Error bars show the range of mean mortality across three censuses. Background mortality from  
 341 FATES simulations is shown with orange bars, damage dependent mortality is shown with green  
 342 bars, and carbon starvation mortality with purple bars.  
 343  
 344  
 345